Published online 10 November 2010 *Nucleic Acids Research, 2011, Vol. 39, No. 6* ***2271–2285***
doi:10.1093/nar/gkq1124

The AddAB helicase–nuclease catalyses rapid and processive DNA unwinding using a single Superfamily 1A motor domain

Joseph T.P. Yeeles[1], Emma J. Gwynn[1], Martin R. Webb[2] and Mark S. Dillingham[1,*]

[1]DNA-Protein Interactions Unit, School of Biochemistry, Medical Sciences Building, University of Bristol, University Walk, Bristol, BS8 1TD and [2]MRC National Institute for Medical Research, Mill Hill, London, NW7 1AA, UK

Received August 10, 2010; Revised October 18, 2010; Accepted October 20, 2010

ABSTRACT

The oligomeric state of Superfamily I DNA helicases is the subject of considerable and ongoing debate. While models based on crystal structures imply that a single helicase core domain is sufficient for DNA unwinding activity, biochemical data from several related enzymes suggest that a higher order oligomeric species is required. In this work we characterize the helicase activity of the AddAB helicase–nuclease, which is involved in the repair of double-stranded DNA breaks in *Bacillus subtilis*. We show that the enzyme is functional as a heterodimer of the AddA and AddB subunits, that it is a rapid and processive DNA helicase, and that it catalyses DNA unwinding using one single-stranded DNA motor of 3′→5′ polarity located in the AddA subunit. The AddB subunit contains a second putative ATP-binding pocket, but this does not contribute to the observed helicase activity and may instead be involved in the recognition of recombination hotspot sequences.

INTRODUCTION

Helicases are a ubiquitous class of enzyme involved in many different aspects of nucleic acid metabolism including DNA replication, repair and recombination. They are molecular motor proteins that couple the energy of ATP binding and hydrolysis to movement along DNA and concomitant separation of the duplex into its component single strands. Originally, helicases were categorized into several families and Superfamilies (SF) based on their primary structures (1), and this classification has been developed to take into account mechanistic aspects of their activity (1,2). For example, many helicases have been shown to translocate with a defined polarity with respect to one strand of the DNA. Enzymes moving towards the 5′-end of single-stranded DNA (ssDNA) are designated class A, whereas members of class B move towards the 3′-end. Despite containing conserved helicase motifs, many enzymes that have been classified as helicases do not actually catalyse duplex DNA unwinding, but are molecular motors that translocate on DNA to perform functions such as chromatin remodelling and DNA restriction (2).

Helicase Superfamily 1 (SF1) is defined by the presence of several conserved regions in the primary amino acid sequence (1,2). Members of this group share a catalytic core of tandem RecA-like domains encoded within a single polypeptide, and this is also a feature of the SF2 class of helicase. Many of the conserved amino acid residues line a groove formed between the RecA-like domains and create an ATP-binding pocket (3,4). Cycles of ATP binding and hydrolysis at this site cause the cleft between the domains to open and close. This domain movement is thought to drive unidirectional translocation along ssDNA using an inchworm mechanism [Reviewed in (2,5)]. This model is based principally upon crystal structures of the related SF1A enzymes PcrA and UvrD in different nucleotide bound states and is also supported by certain biochemical analyses (6–9). It envisages that a single helicase core unit (i.e. a monomer) is sufficient for processive unwinding (Figure 1A). Furthermore, it was suggested that the key features of this mechanism were conserved in the SF1B enzyme RecD2, although details of the mode of interaction with, and translocation along, ssDNA differ for the A and B class of SF1 helicase (10). In spite of this, a long-standing debate has arisen around the simple and contradictory observation that many SF1 helicases (including the SF1A enzymes Rep, PcrA, UvrD and the SF1B enzyme Dda) catalyse little or no duplex DNA unwinding under conditions that favour monomeric

*To whom correspondence should be addressed. Tel: +44 117 3312159; Fax: +44 117 3312168; Email: mark.dillingham@bristol.ac.uk
Present address:
Joseph T.P. Yeeles, Molecular Biology Program, Memorial Sloan-Kettering Cancer Center, New York, NY, USA.

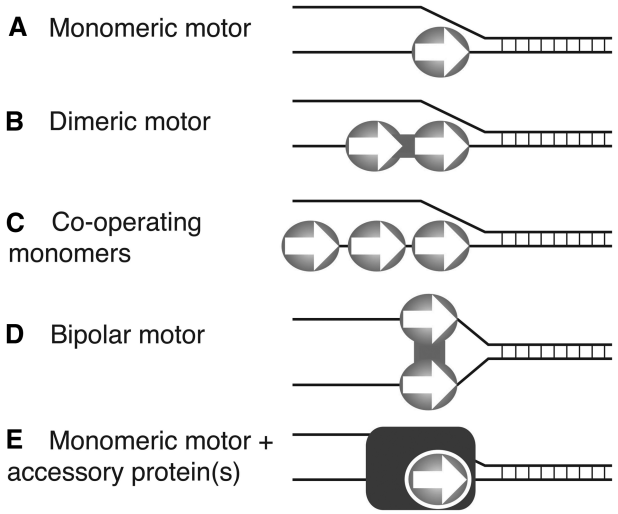

Figure 1. DNA unwinding models for SF1 DNA helicases. Various models have been suggested for how SF1 helicases may catalyse DNA unwinding. They have been proposed to function as both monomers (**A**) and dimers (**B**). It has also been shown that multiple SF1 helicase monomers may cooperate to facilitate unwinding of the same DNA molecule (**C**). A bipolar helicase (e.g. RecBCD) utilizes two SF1 helicase motors of opposite polarity to catalyse processive DNA unwinding (**D**). The DNA unwinding activity of many SF1 enzymes is enhanced through interactions with specific partner proteins (**E**). SF1 helicase domains are represented by ovals with white arrows and accessory protein(s) are shown as squares. See the text for references and further discussion of these mechanisms.

species (11–16). This conclusion is based upon experiments that employ oligonucleotide-based substrates consisting of a short duplex region of DNA flanked by a ssDNA tail that is required for helicase loading. In some cases (12,14–16), under single turnover conditions there is an absolute requirement for at least two helicase polypeptides to be loaded at the ssDNA tail to observe unwinding. In other cases (13,17), multiple monomers are required for optimal activity but limited unwinding is still observed with the monomeric species. As a result of such experiments, models have been proposed whereby co-operation or self-association between helicase monomers is required for optimal duplex DNA unwinding (Figure 1B and C). For example, Rep, UvrD and PcrA are all proposed to self-associate to form active dimeric helicases, whereas multiple monomers of Dda are thought to co-operate in order to increase helicase activity (12,13,15,16). In the former cases, however, it is not clear that direct protein–protein interactions are required for this activation of apparent helicase activity. Another possible weakness of these studies is that they do not address the physiological significance of the reaction being studied *in vitro*. This point may be particularly pertinent when one considers that the apparent helicase activity of many isolated SF1 enzymes is poor, but is dramatically activated by association with partner proteins. Interactions with self and non-self partner proteins seem to be a common feature of SF1 helicase function, and these interactions serve to target or regulate helicase activity (2,18). The UvrD helicase functionally interacts with the mismatch repair protein MutL and is stimulated by the nucleotide excision repair proteins UvrAB (19,20). Likewise, the accessory protein CisA enhances the processivity of Rep (21). Remarkably, interaction between PcrA and the plasmid replication initiator protein RepD stimulates PcrA helicase activity to such an extent that it is capable of processively unwinding plasmid length DNA (i.e. thousands of base pairs), despite being unable to separate relatively short duplexes (tens of base pairs) in isolation (22,23). The TraI helicase is an exceptional case: it catalyses a very rapid and processive DNA helicase reaction in the monomeric form and in the absence of accessory proteins *in vitro*. However, this behaviour may be explained by the fact that TraI is a large (192 kDa) protein that contains accessory DNA-binding domains which may enhance processivity (24) (Figure 1E). Taken together, these observations show that SF1 helicases may operate by a range of different mechanisms *in vitro*, and raise the possibility that *cis*-acting accessory domains or *trans*-acting partner proteins may be frequently or perhaps even always, necessary as activators of helicase activity *in vivo*. In spite of this, the molecular basis for this activation remains relatively poorly studied [although studies in Rep helicase highlight an important role for a *cis*-acting auto-inhibitory domain (12)]. Furthermore, the mechanism and oligomeric state of helicases within the context of multi-protein machines has not been widely investigated.

Bacterial helicase–nuclease complexes that initiate recombinational repair from broken DNA ends are useful model systems for *in vitro* mechanistic studies of helicase activity. They can be purified as stable multi-protein complexes (i.e. without missing components) and catalyse a potent DNA unwinding and degradation reaction *in vitro* that closely reflects their known *in vivo* function in the resection of free DNA ends. Helicase–nuclease complexes target broken duplex DNA ends and then processively unwind DNA whilst simultaneously cleaving the nascent 3′- and 5′-terminated strands. Following recognition of specific regulatory sequences known as Chi (**C**rossover **h**otspot **i**nstigator) sites, cleavage of the 3′-terminated strand is attenuated while the enzymes continue to translocate along DNA and degrade the 5′-terminated strand. The resulting 3′-ssDNA tail is bound by the homologous pairing enzyme RecA, to promote the faithful repair of the DNA lesion via homologous recombination (25,26). There are two structural classes of helicase–nuclease complexes (Figure 2), referred to as AddAB- and RecBCD-type enzymes. RecBCD is a bipolar DNA helicase containing two SF1 helicase motors that are located in the RecB and RecD subunits within the heterotrimeric complex (27,28). It unwinds DNA at rates of up to ~1600 bp/s with a processivity in excess of 30 000 bp (25,29–33). This powerful activity results in part from the combined activity of the two motor domains of the RecBCD complex (Figure 1D) (30). In contrast, AddAB complexes contain only a single complete set of helicase motifs (in the AddA subunit) and it was suggested that the AddAB complex can function as a helicase using only a single motor subunit (26,34). However, the oligomeric state (and therefore the number of AddA motor domains) in the functional complex has never been determined. Moreover, a large subset of AddAB enzymes

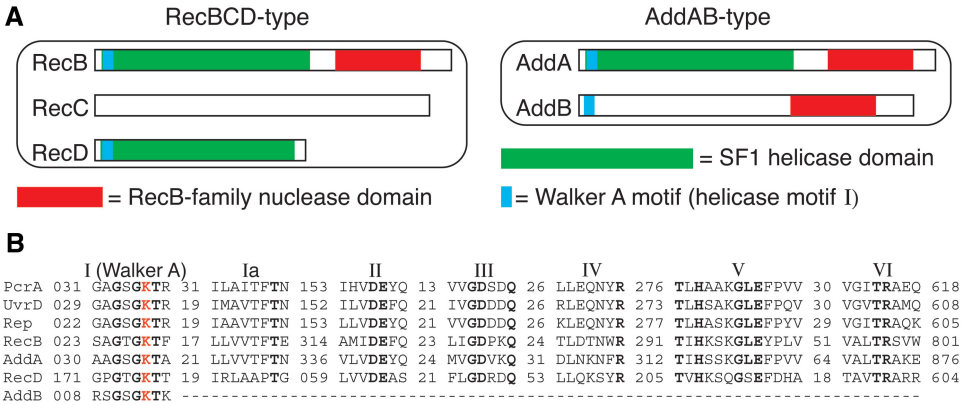

Figure 2. RecBCD- and AddAB-type helicase–nucleases contain Superfamily 1 helicase domains. (**A**) Primary structure diagrams highlighting the positions of the SF1 helicase domains and Walker A motifs in RecBCD- and AddAB-type helicase–nuclease enzymes. (**B**) Sequence alignment of the seven SF1 helicase motifs (1) of *E. coli* UvrD, Rep, RecB and RecD and *B. subtilis* PcrA and AddA. *B. subtilis* AddB has a conserved Walker A motif (helicase motif 1) but apparently lacks the remaining helicase motifs. Conserved residues are shown in bold.

(including the enzyme from *Bacillus subtilis* studied here) contain a second putative ATP-binding site, by virtue of a Walker A motif found near the N-terminus of the AddB subunit (35).

In this study, we present a biochemical characterization of the helicase activity associated with an AddAB-type helicase–nuclease. We show that AddAB is active as a heterodimeric complex and that it catalyses rapid and processive DNA unwinding using a single helicase motor with a 3′→5′ ssDNA translocation polarity. The AddA subunit harbours the helicase activity, and is able to unwind short DNA substrates in the absence of AddB, albeit with a complete loss of the physiological specificity for DNA ends. Our results strongly suggest that the putative ATP-binding pocket in AddB does not play a role as a secondary DNA motor, but that it may instead facilitate the recognition of the recombination hotspot sequence Chi.

MATERIALS AND METHODS

Protein expression and purification

AddAB and $AddA^{N}B^{N}$ were prepared as described previously (36,37). The $AddA^{N}B^{N}$ protein contains two mutations ($AddA^{D1172A}$ and $AddB^{D961A}$) that effectively eliminate the nuclease activity of the AddAB complex (37). AddAB concentrations were determined using the Bradford assay (Biorad), and all stated concentrations refer to the heterodimeric complex ($AddA_1AddB_1$). PcrA was purified as described previously (38). Dda helicase was a gift from Kevin Raney (University of Arkansas). $AddA^{N}$ ($AddA^{D1172A}$ mutant) and $AddA^{N,H}$ ($AddA^{K36A,D1172A}$ double mutant) expression vectors were generated by cloning mutant *adda* genes into pET15b using the enzymes NdeI and XhoI, enabling the proteins to be expressed with an N-terminal hexa-histidine tag. Cells were grown at 37°C in Luria broth supplemented with 50 μg/ml carbenicillin to an OD_{600} of 0.5. Following induction with 1 mM IPTG, cultures were incubated for a further 3 h at 27°C prior to harvest and resuspension in 50 mM Tris–Cl pH 7.5, 10% (w/v) sucrose. Cells were lysed by sonication and the lysate was loaded onto a 5 ml HisTrap FF column (GE Healthcare) equilibrated in B-buffer (20 mM Tris–Cl pH 7.5, 1 mM EDTA, 0.1 mM DTT) + 500 mM NaCl + 25 mM imidazole. His-tagged proteins were eluted with a 30 column volume gradient from 25 to 500 mM imidazole. The peak fractions were dialysed against B buffer + 50 mM NaCl prior to MonoQ chromatography. Proteins were applied to a 1 ml MonoQ column (GE Healthcare) equilibrated in B-buffer + 200 mM NaCl and were subsequently eluted with a 30 column volume gradient from B-buffer + 200 mM NaCl to B-buffer + 600 mM NaCl. Peak fractions were pooled and buffer exchanged using a 5 ml Hi-Trap desalting column (GE Healthcare) into B-buffer + 100 mM NaCl + 10% (v/v) glycerol for storage at −80°C. AddA concentrations were determined spectrophotometrically using the theoretical extinction coefficient of 135 460/M/cm at 280 nm. The fluorescent biosensors MDCC-PBP and DCC-SSB were prepared as described previously (39,40).

DNA substrates

All oligonucleotides used in this study were obtained from Eurofins MWG Operon. Substrates for helicase assays were prepared as described previously by annealing ^{32}P-labelled 30-base oligonucleotides to unlabelled 30- or 60-base oligonucleotides (37). The substrates generated are illustrated in Supplementary Table S1. The sequences of the oligonucleotides used for streptavidin displacement assays were as follows, where X indicates the presence of a biotin-dT nucleotide: 5bio45 5′-GXA CGT ATT CAA GAT ACC TCG TAC TCT GTA CTG ACT CGG ATC CTA-3′ and 3bio45 5′-GTA CGT ATT CAA GAT ACC TCG TAC TCT GTA CTG ACT CGG ATC CXA-3′.

DNA substrates for electrophoretic mobility shift assays (EMSA) and AUC experiments were generated by annealing two 19-base oligonucleotides to form a molecule with a 15-bp duplex region and four-base 3′-overhangs. The oligonucleotide sequences are shown below: Bind15_1 5′-CCG CCT CTT GGC CGA TTC A- 3′ and

Bind15_2 5′-GTT TGG CGG AGA ACC GGC T - 3′. The bind_15 duplex was 5′-labelled with ^{32}P as described previously (37). Fluorescent duplex substrates for AUC experiments contained a single Cy5 fluorophore attached to the 5′-terminus of the Bind15_1 oligonucleotide. The substrate was generated by annealing equimolar (50 μM) Bind15_1Cy5 and Bind15_2 in 5 mM potassium phosphate pH 6.8 and 200 mM KCl. Unannealed ssDNA was removed by ResourceQ (GE healthcare) chromatography. The DNA concentration was calculated using the extinction coefficient of 250 000/M/cm for Cy5 absorbance at 649 nm.

The 389-bp substrate used in stopped flow experiments was generated by PCR with one biotinylated primer using the plasmid pSP73-JY10 as template essentially as described (41). PCR products were purified using a PCR clean-up kit (Qiagen) and isopropanol precipitation. The DNA concentration was calculated using the nucleotide extinction coefficient of 6500/M/cm at 260 nm.

EMSA

All EMSA assays were carried out in a buffer containing 25 mM Tris–acetate pH 7.5, 2 mM magnesium acetate, 1 mM DTT and 2.5% (w/v) Ficoll 400. The buffer was supplemented with 100 mM sodium acetate where indicated in the figure legends. DNA and proteins at the indicated concentrations were incubated in the above buffer for 10 min at room temperature prior to electrophoresis at 120 V through 8% (w/v) polyacrylamide gels in TBE. The resulting gels were dried on DEAE paper and visualized using a Typhoon 9400 phosphorimager (Molecular Dynamics). Gels with Cy5-labelled DNA were directly visualized using a Typhoon 9400 imager in fluorescence mode. Data was quantified using ImageQuant software and fit to Equation (1) that describes the binding of a ligand to a single site on a protein:

$$Y = \frac{\left(0.5 \times \left((X+K_d+nZ) - \sqrt{(X+K_d+nZ)^2 - (4XnZ)}\right)\right)}{0.01nZ} \quad (1)$$

where Y is the percentage of bound ligand, X is the total AddAB concentration, Z is the total DNA concentration, K_d is the dissociation constant, and n is the number of DNA molecules bound by each AddAB enzyme. We have shown previously that the K_d value for AddAB binding to DNA ends is extremely tight (<50 pM) (42) and the experiments performed here have greater than two orders of magnitude higher DNA concentrations. Therefore, AddAB-binding stoichiometries ($1/n$) were calculated from Equation (1) by floating the value of n, constraining the K_d to 50 pM and setting the DNA concentration (Z) to the relevant experimental value.

Analytical ultracentrifugation

Sedimentation equilibrium ultracentrifugation was performed in an Optima XL-A analytical ultracentrifuge (Beckman). All analytical ultracentrifugation experiments were conducted at 4°C in a buffer containing 25 mM Tris–acetate pH 7.5, 2 mM magnesium acetate and 100 mM sodium acetate. As the experiments required the protein to be incubated with DNA for long periods of time, the nuclease deficient enzyme AddA^{N}B^N was utilized in all AUC experiments to avoid degradation of the substrate. For experiments containing AddA^{N}B^N alone, data were collected at 280 nm. When the samples contained the Cy5Bind15 substrate, data were collected at 645 nm in order to monitor the absorbance of the Cy5 fluorophore. The rotor speeds at which the cells were spun were selected according to the molecular weights of the species being investigated, and runs were continued until equilibrium was reached, at which point the distribution of the sample in the cell is invariant with time. Absorbance scans were taken at 4 h intervals and equilibrium was identified by overlaying consecutive 4 h scans. In the absence of DNA, ultracentrifugation was carried out at 4000 rpm with 1, 2 and 2.5 μM samples of AddA^{N}B^N. For experiments containing solely the Cy5Bind15 substrate, data were collected with 1 μM DNA at speeds of 18 000, 22 000 and 26 000 rpm. Samples that contained both DNA and enzyme were conducted with 1 μM Cy5Bind15 and 2.5 or 5 μM AddA^{N}B^N as indicated. Centrifugation was carried out at 4000, 5000 and 6000 rpm.

Radial absorption scans were analysed using the Microcal Origin software for AUC (MicroCal) by globally fitting three different absorption scans to single-species fits. In the case of experiments containing DNA only and DNA with AddA^{N}B^N, data from three different rotor speeds were globally fitted. In the case of the AddA^{N}B^N only experiments, the absorption scans from three different protein concentrations at a single rotor speed were globally fit. The baseline values used for fitting, which were fixed in each case, were obtained by over-speeding the cells at the end of the run and taking the average of eight absorption values close to the meniscus. The partial specific volume (vbar) of the protein was calculated from the amino acid sequence using the program SEDNTERP (43), and the same program was also used to calculate the buffer density. A vbar value of 0.57 ml/g was selected for DNA and in the case of DNA and protein together, vbar values were calculated that took into account the proportions of the molecular weight of bound species made up by DNA and protein.

ATP hydrolysis assays

Measurements were made at 25°C in a Cary Eclipse fluorimeter with excitation light at 430 nm and a 465 nm cut-off filter. Standard reactions contained 25 mM Tris–acetate pH 7.5, 2 mM magnesium acetate, 1 mM DTT and 8 μM MDCC-PBP. For ATP titrations the reactions contained 100 μM nucleotides dT_{35} (equivalent to 2.9 μM molecules) and for dT_{35} titrations the ATP concentration was 320 μM. Experiments were initiated by addition of AddAB enzymes to 150 pM. In order to minimize phosphate contamination a 10 mM ATP stock solution, supplemented with 1 mM 7-methyl-guanosine, was treated with 0.025 U/ml purine nucleoside phosphorylase (PNPase) (Sigma) at 25°C for 30 min. PNPase catalyses the phosphorylysis of 7-methyl-guanosine, forming ribose-1-phosphate and

7-methyl-guanine in an essentially irreversible reaction. The rate at which phosphate was added to 7-methyl-guanosine was not significant compared to the binding of phosphate to MDCC-PBP under the experimental conditions used. Data were calibrated by generating a standard curve for phosphate binding to PBP in standard reaction buffer. Initial rates were calculated and were fit to the Michaelis–Menton equation.

Real-time helicase assays

Experiments were performed at 37°C in an SHU-61SX2 stopped-flow fluorimeter with a mercury-xenon lamp (TgK Scientific Limited, Bradford-on-Avon, UK). Excitation light was 436 nm with a 455 nm cut-off filter. All stated concentrations are final after mixing in the reaction chamber. A total of 1 nM DNA was incubated with 10 nM streptavidin in reaction buffer (25 mM Tris–acetate pH 7.5, 2 mM magnesium acetate, 1 mM DTT, 100 μg/ml BSA, 200 nM DCC-SSB monomer). $AddA^{N}B^{N}$ was pre-bound to the DNA at the indicated concentrations for 1 min at room temperature. After a further 1-min equilibration at 37°C in the stopped-flow apparatus, samples were rapidly mixed against equal volumes of 0.5 mM ATP and 100 nM $AddA^{H}B$ in reaction buffer. The fluorescence signal obtained was calibrated using heat-denatured DNA. Amplitude data were fit to a modified version of Equation (1), which includes a scaling factor (F_{max}) for the maximum fluorescence increase under saturating conditions [Equation (2)]. Stoichiometry values ($1/n$) were obtained with the K_d value constrained to 50 pM.

$$Y = \frac{F_{max}\left(\left(0.5 \times \left((X+K_d+nZ) - \sqrt{(X+K_d+nZ)^2 - (4XnZ)}\right)\right)\right)}{0.01nZ} \quad (2)$$

dsDNA end processing reactions

Reactions were performed as described previously (37). The reaction buffer contained 25 mM Tris–acetate pH 7.5, 0.25 mM magnesium acetate, 1 mM DTT, 1.6 nM molecules ^{32}P-labelled pADGF0, 2 μM *Escherichia coli* SSB (monomer) and 0.5 nM wild-type or mutant AddAB enzymes as indicated.

DNA processivity assay

AddAB processivity assays were based on a published method (30). All measurements were taken in a Cary Eclipse fluorescence spectrophotometer (Varian) at 37°C. Phage λ DNA (~50 kb) was used in these experiments as it provides a suitably long substrate for assessing processivity. Prior to conducting the assay, diluted λ DNA was heated to 65°C for 10 min in order to disrupt the 12-base complementary 5′-overhangs (cos sites) at either end of the DNA molecule, and then stored on ice. Dye-displacement assays were conducted using excitation and emission wavelengths of 344 and 487 nm, respectively. DCC-SSB assays were performed using excitation and emission wavelengths of 430 and 475 nm, respectively. All concentrations quoted below are final, after mixing of the components to initiate the reactions. Reaction mixtures contained 25 mM Tris–acetate pH 7.5, 2 mM magnesium acetate, 100 μg/ml BSA, 0.05 nM λ DNA molecules, 2 nM AddAB enzymes and either 1 μM DCC-SSB (DCC-SSB assay) or 1 μM *E. coli* SSB (monomer) and 300 nM Hoechst 33258 (Dye-displacement assay). DNA unwinding was initiated by adding either 0.5 mM ATP or 0.5 mM ATP and 50 nM $AddA^{H}B$ as indicated. Unwinding signals reached a stable plateau by 3.5 min, indicating that reactions had reached completion. The amplitudes of unwinding were therefore calculated from at least two repeats by taking the amplitude of the fluorescence change at 3.5 min. The fluorescence signals were calibrated using heat-denatured λ DNA.

Streptavidin displacement assay

Streptavidin displacement assays were based on the method of Morris and Raney (44). All concentrations are final concentrations after mixing. A total of 5 nM 5′ ^{32}P-labelled substrate oligonucleotides were incubated for 5 min at room temperature with 400 nM streptavidin in 50 mM Bis–Tris–acetate pH 6, 2 mM magnesium acetate and 25 mM NaCl. Reactions were initiated by mixing the above solution with an equal volume of buffer containing either 500 nM $AddA^{N}$ or $AddA^{N,H}$ as indicated, 4 mM ATP, 8 μM biotin, 50 mM Bis–Tris–acetate pH 6, 2 mM magnesium acetate and 25 mM NaCl. Reactions were incubated at 37°C for the indicated times and were then terminated with an equal volume of 300 mM EDTA, 400 mM NaCl and 30 μM poly(dT). The products were separated on 10% gels at 100 V and were processed as described for the EMSA assays.

Strand-displacement helicase assay

Strand-displacement helicase assays were based on the method of Matson *et al.* (45). Standard reactions contained: 25 mM Tris–acetate pH 7.5, 2 mM magnesium acetate, 1 mM DTT, 0.5 mM ATP and 10 nM ^{32}P-labelled substrate DNA. The reactions were initiated by addition of the indicated enzymes to concentrations of 10 nM for $AddA^{N}$ / $AddA^{N,H}$ and 200 nM for PcrA / Dda. Following incubation at 20°C for the indicated times, 10 μl aliquots were removed and quenched in 10 μl 2× stop buffer, which contained 200 mM EDTA, 1% SDS, 10% (w/v) Ficoll 400 and 100 nM of an unlabelled form of the oligonucleotide that is equivalent to the one that is ^{32}P-labelled in the dsDNA substrate. The unlabelled oligonucleotide is included in the stop buffer to prevent the separated radiolabelled strand from reforming duplex by reannealing prior to electrophoresis. Products were separated on 15% polyacrylamide gels in 1× TBE and were processed as described for EMSA assays.

Exonuclease chase assay

Assays were performed using a published method (46). A total of 10 μM nucleotides (1.6 nM molecules) tailed 5′-^{32}P-labelled pADG6406-1 were processed by 3.2 nM AddAB enzymes at 37°C in a buffer composed of 25 mM Tris–acetate pH 7.5, 2 mM magnesium acetate, 1 mM DTT, 1 mM ATP and 2 μM *E. coli* SSB. Following 30 s incubation, the 3′→5′ ssDNA exonuclease,

Exonuclease I (ExoI) (NEB) was added to a final concentration of 0.8 U/μl. Aliquots were removed at the indicated time points and were quenched and processed as described previously (37).

RESULTS

A single AddAB heterodimer binds tightly to a dsDNA end

Previous studies have demonstrated that the AddAB helicase–nuclease is a stable heterodimer (i.e. $AddA_1AddB_1$) in solution and that it displays a sub-nanomolar affinity for dsDNA ends, which are the physiological substrate for the enzyme complex (36,37). However, the oligomeric state of the DNA-bound complex has never been investigated. Therefore we studied the binding of AddAB to a 15-bp duplex with four-base 3′-overhangs (Bind15) using EMSA and analytical ultracentrifugation (AUC). The Bind15 DNA was first shown to be a *bona fide* substrate for AddAB helicase activity (Supplementary Figure S1). EMSA assays were then conducted using DNA concentrations significantly in excess of the dissociation constant for the AddAB:Bind15 interaction (Figure 3A). The K_d value for this interaction is too tight to be measured accurately but was determined by EMSA to be <50 pM (42). Binding of excess AddAB to 10 nM substrate DNA shifts the position of Bind15 to a single band in the native gel. The gel position of essentially all the DNA is shifted by the AddAB complex at a stoichiometry equivalent to one AddAB complex ($AddA_1AddB_1$) per DNA molecule, and no supershift occurs at higher AddAB concentrations. This result suggests that a single AddAB enzyme binds to Bind15, despite the presence of two dsDNA ends per substrate. The data can be explained if, due to the short length of the substrate, the duplex region is only long enough to accommodate AddAB binding to one end of the DNA molecule. In agreement with this hypothesis, lengthening the duplex region to 50 bp allows the formation of a second, more slowly migrating band, indicating that AddAB enzymes are likely to bind simultaneously to both ends of the substrate when the duplex region is long enough to permit two independent end-binding events (data not shown). Further EMSA titrations were conducted with three different DNA concentrations, all significantly in excess of the dissociation constant (Figure 3B). At all three DNA concentrations, there is a linear increase in the amount of DNA–Protein complex with increasing total AddAB concentration, until a sharp break-point is reached at close to 100% binding. The data were fit to a single-site binding equation [Equation (1)]. With the K_d values constrained to 50 pM (the known upper bound for the dissociation constant), the apparent stoichiometry of the DNA:protein interaction was determined by fitting to Equation (1). This procedure returned AddAB:Bind15 stoichiometries of; 1.02:1, 1.00:1 and 1.04:1 for experiments performed at three different DNA concentrations. These data suggest that AddAB binds to Bind15 as a single heterodimer, but EMSA experiments should be viewed with caution as they are sensitive to errors in both the DNA and enzyme concentrations. Indeed, stoichiometry values were determined for a range of independent AddAB preparations and were found to vary between 1.0:1 and 1.5:1 (data not shown). This variation can be at least partially attributed to a relatively unstable iron–sulphur cluster in the AddB subunit which is known to be essential for dsDNA end-binding (36). Therefore, to support the EMSA analysis, samples were further studied

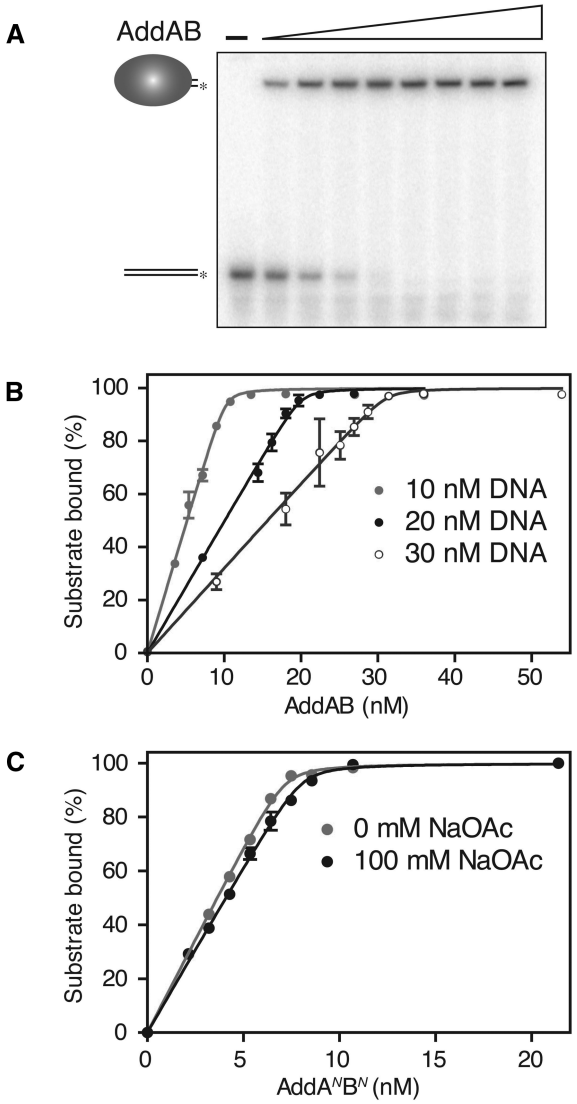

Figure 3. EMSA analysis of the stoichiometry of AddAB binding to dsDNA ends. (**A**) EMSA assays were conducted with 10 nM ^{32}P-labelled Bind15 substrate in the standard dsDNA end-binding buffer with varying AddAB concentrations (0, 3.6, 7.2, 9, 10.8, 13.5. 18, 27, 36 nM). The positions of the free DNA and AddAB:DNA complex are indicated. (**B**) EMSA experiments were conducted with 10, 20 or 30 nM Bind15 as indicated. The proportions of the substrate bound by varying concentrations of AddAB were calculated for two independent repeats. Error bars represent the standard error of the mean (SEM). The data were fit to Equation (1). (**C**) Quantification of EMSA data characterizing the binding of $AddA^NB^N$ to Cy5Bind15. Samples contained 5 nM Cy5Bind15 in the standard dsDNA end-binding buffer in the presence or absence of 100 mM sodium acetate. The proportion of the bound substrate was calculated for two repeats. The error bars represent the SEM and the data were fit to Equation (1).

by AUC using a modified Bind15 substrate labelled with a single Cy5 fluorophore. The Cy5 label absorbs at long wavelengths, enabling the sedimentation profile of the DNA to be monitored independently from that of the protein. To limit nucleolytic degradation of the DNA substrate during the long AUC runs, experiments were conducted using the nuclease-deficient AddAB enzyme AddA^{N}B^N, which displays wild-type dsDNA end binding, helicase and Chi-recognition activities (37). The experimental conditions used for AUC were further modified to include 100 mM sodium acetate, which was required to reduce charge effects caused by the presence of DNA. Therefore, prior to conducting the AUC experiments, the stoichiometry for AddA^{N}B^N binding to Cy5Bind15 was investigated in the presence and absence of 100 mM sodium acetate (Figure 3C). The stoichiometry is not significantly influenced by the presence of sodium acetate and returns an apparent value of 1.5 AddA^{N}B^N:1 DNA.

Sedimentation equilibrium experiments were first performed in the absence of DNA, with 1 μM, 2.5 μM and 5 μM AddA^{N}B^N. Data was collected at 280 nm for the three enzyme concentrations and globally fit to a model that describes the sedimentation of a single monodisperse species (Supplementary Figure S2) to yield an apparent molecular weight ($M_{w,app}$) of 283 kDa (Table 1). Given that the theoretical molecular weight of a single AddAB heterodimer is 275 kDa, these data confirm our previous gel filtration studies (36) which suggested that AddAB is a heterodimer (AddA$_1$AddB$_1$) in the absence of DNA. Samples containing Cy5Bind15 DNA were then analysed at 649 nm in the presence and absence of AddA^{N}B^N. In the absence of AddA^{N}B^N, data from three different sedimentation speeds were globally fit to give an $M_{w,app}$ of 11.5 kDa, which is in good agreement with the theoretical value of 12.1 kDa (Table 1 and Supplementary Figure S2). To assess the molecular weight of the AddAB:Cy5Bind15 complex, 1 μM DNA was incubated with either 2.5 or 5 μM AddA^{N}B^N and the data (collected at 649 nm) from three sedimentation speeds were globally fit to yield $M_{w,app}$ values of 276 kDa and 268 kDa, respectively (Table 1 and Supplementary data). The $M_{w,app}$ values measured in this way are insensitive to any small errors in the AddA^{N}B^N and DNA concentrations and confirm that a single AddAB heterodimer binds to a single Bind15 substrate.

Table 1. Summary of the apparent molecular weight values derived from AUC experiments

AUC sample	Molecular weight (kDa)	
	Theoretical	AUC ($M_{w,app}$)
AddA^{N}B^N	275	283
Cy5Bind15 DNA	12	11.5
AddA^{N}B^N–Cy5Bind15 complex (2.5-fold excess AddA^{N}B^N)	287	277
AddA^{N}B^N–Cy5Bind15 complex (5-fold excess AddA^{N}B^N)	287	268

Analytical ultracentrifugation analysis is associated with an error of around ±5% in the determination of the molecular weight [for discussions see (43,63)].

The AddAB heterodimer is the active form of the enzyme complex for dsDNA unwinding

Having established that a single AddAB heterodimer binds to Bind15, we next sought to determine the oligomeric state of the enzyme during processive dsDNA unwinding using a single-turnover real-time helicase assay. The assay employs a recently developed bio-sensor to monitor the production of ssDNA in real-time (39). DCC-SSB is a coumarin-modified *E. coli* SSB protein that displays a 4- to 6-fold fluorescence increase upon binding to ssDNA (39). A 389-bp DNA substrate was used which only contains a single free DNA end for AddAB binding (Figure 4A) and three correctly-oriented Chi sites, separated by 9-bp regions of non-specific DNA, the first of which is 55 bp from the free end. The assays were conducted with the nuclease-deficient AddA^{N}B^N protein to avoid the complications associated with substrate degradation. AddA^{N}B^N was pre-bound to the

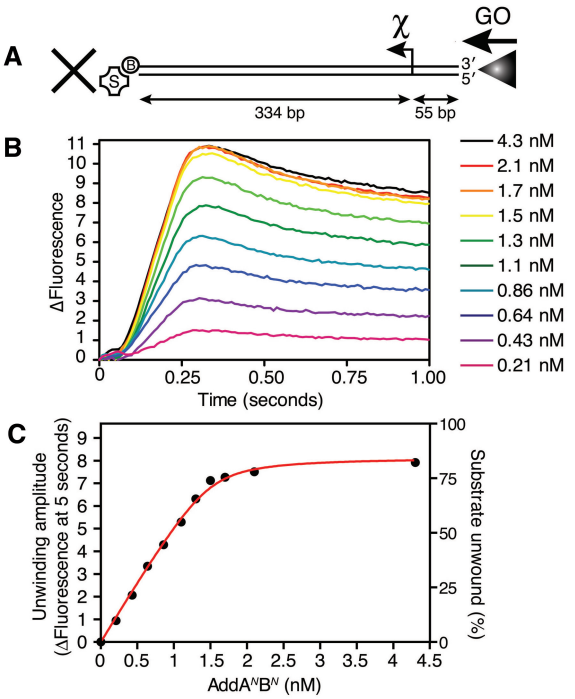

Figure 4. The AddAB heterodimer is the active form of the enzyme during dsDNA unwinding. (**A**) Schematic representation of the DNA substrate used in real time helicase assays. The position of a 5′-biotin is denoted by a B, while S represents a streptavidin molecule. (**B**) Fluorescent SSB assays were conducted in the standard buffer with a DCC-SSB concentration of 200 nM. AddA^{N}B^N enzymes were pre-bound at the indicated concentrations to the substrate DNA (1 nM) that was blocked at the distal end with streptavidin. Substrate unwinding was initiated by rapid mixing of the DNA:AddA^{N}B^N complex against an equal volume of 0.5 mM ATP and 100 nM AddA^{H}B trap in reaction buffer. The data have been normalized by subtracting the initial fluorescence values for the individual traces. (**C**) The final amplitude of unwinding (measured as a change in fluorescence at 5 s) is plotted for each AddA^{N}B^N concentration. The fluorescence was calibrated using heat-denatured substrate DNA and data were fit to Equation (2).

productive binding site and the distal end of the DNA substrate was blocked with a streptavidin molecule bound to a biotin moiety (Supplementary Figure S3A). To ensure single-turnover unwinding conditions, an AddAB mutant enzyme (AddA^{H}B) that can bind to, but not unwind, DNA (37) was employed as a 'trap' that largely prevents the binding or rebinding of AddA^{N}B^{N} to the DNA substrate following the addition of ATP (Supplementary Figure S3B). The experiments were conducted using 1 nM DNA substrate (equivalent to 1 nM AddAB-binding sites) and varying concentrations of AddA^{N}B^{N} were pre-bound to the DNA substrate. Unwinding was initiated with ATP and a large excess of AddA^{H}B. For all concentrations of AddA^{N}B^{N}, there was a rapid increase in fluorescence for approximately 0.3 s, which corresponds to DCC-SSB binding to the nascent ssDNA produced by the processive activity of AddA^{N}B^{N} helicase in a single turnover (Figure 4B). This phase was followed by a gradual decrease in fluorescence until the signal reaches a plateau after several seconds (Supplementary Figure S4). The slow post-unwinding decrease in fluorescence is probably the result of the DCC-SSB probe switching between binding modes on the ssDNA reaction products as has been demonstrated previously (47). This switching is likely to occur at <5% the rate of the initial binding and so is unlikely to influence substantially the observed initial rate (47). Regardless of this complication, the duration of the unwinding phase (~0.3 s) suggests a very rapid translocation rate (on the order of 1000 bp s^{-1}), in broad agreement with other measurements (36,48).

The amplitude of the total fluorescence increase at the plateau is proportional to the AddA^{N}B^{N} concentration until a sharp break point is reached at an AddA^{N}B^{N} concentration of ~1.5 nM (Figure 4C). At this saturation point, ~85% of the DNA substrate is being unwound in a single turnover. The data in Figure 4C were fit to Equation (2) to determine an apparent stoichiometry of 1.50 AddAB:1 DNA. Together with our previous observations that the apparent stoichiometry for formation of the AddA^{N}B^{N}-Cy5Bind15 complex is 1.43:1 (Figure 3C), and that this complex contains a single AddA^{N}B^{N} heterodimer bound to Cy5Bind15 (Table 1 and Supplementary Figure S2), the helicase assay shows unequivocally that an AddAB heterodimer is the active form of the enzyme during dsDNA unwinding.

The AddAB heterodimer is a highly processive DNA helicase powered by a single motor in the AddA subunit of the complex

The AddA subunit of the AddAB complex contains all of the SF1 helicase motifs, strongly suggesting that the subunit is involved in AddAB helicase activity (Figure 2). However, the AddB subunit also has an intact Walker A motif (equivalent to helicase motif 1), raising the possibility that it may bind ATP and/or function as a second helicase motor. Note however that it apparently lacks several other motifs that are characteristic of SF1/2 helicases (Figure 2). In order to characterize the putative AddA helicase activity, and to assess the potential functions of the AddB Walker A motif, we studied three mutant AddAB enzymes in which the conserved Walker A lysine residues of either or both subunits were substituted for alanine. It is well established that this mutation very substantially reduces ATP binding and/or hydrolysis in several different classes of ATPase (49). The AddA^{K36A}B, AddAB^{K14A} and AddA^{K36A}B^{K14A} complexes, hereafter called AddA^{H}B, AddAB^{H} and AddA^{H}B^{H}, respectively, will be referred to collectively as 'Walker A mutants'. The three Walker A mutants were purified to near homogeneity using the same procedure as for wild-type AddAB. The mutant enzymes behaved in an identical manner to wild-type AddAB during purification and display indistinguishable dsDNA end binding properties to AddAB (data not shown), suggesting that the point mutations do not affect the tertiary or quaternary structure of the mutant enzymes.

To assess the relative contributions of the AddA and AddB subunits to the overall ATPase activity of the AddAB complex, we measured the DNA-dependent ATPase activity of wild-type AddAB and the Walker A mutants using a fluorescent probe for the production of inorganic phosphate (50). Wild-type AddAB displays a k_{cat} for ATP hydrolysis of 88 s^{-1} and a K_m (ATP) of 6.16 μM (Table 2). As reported previously, this activity is strongly stimulated by the presence of ssDNA, with the apparent affinity for dT$_{35}$ ssDNA (K_{DNA}) calculated to be 188 nM nucleotides (equivalent to 5.4 nM molecules; Table 2). AddAB^{H} displays very similar characteristics, with a k_{cat} of 101/s, K_m of 6.60 μM and a K_{DNA} of 223 nM nucleotides (equivalent to 6.4 nM molecules). This suggests that the putative ATP-binding pocket of AddB does not contribute significantly to the ATPase activity associated with the AddAB complex. In contrast, and in agreement with previous studies (51), both of the enzymes with mutations in the AddA Walker A motif (AddA^{H}B and AddA^{H}B^{H}) display dramatically impaired ATPase activity, and it was not possible to obtain a full set of kinetic parameters. However, at concentrations of ATP and ssDNA that are saturating for wild-type AddAB, turnover rates of 4.6/min and 2.6/min were measured for AddA^{H}B and AddA^{H}B^{H} respectively. The difference in these rates is reproducible,

Table 2. Kinetic parameters for the ssDNA-stimulated ATPase activities of wild-type and Walker A mutant AddAB enzymes

Enzyme	k_{cat} [a]	K_M (ATP)	K_{DNA} (dT$_{35}$ nucleotides)
AddAB	88.4/s ± 0.7	6.16 μM ± 0.23	188 nM ± 20
AddAB^{H}	101/s ± 1	6.60 μM ± 0.29	223 nM ± 29
AddA^{H}B	4.64/min ± 0.08	N/D	N/D
AddA^{H}B^{H}	2.60/min ± 0.14	N/D	N/D

Values for AddAB and AddAB^{H} were derived by fitting data from ATP and dT$_{35}$ titrations to the Michaelis–Menton equation and the errors shown are the standard errors from the fits (data not shown).
[a]The k_{cat} values for AddAB and AddAB^{H} were derived from ATP titrations at saturating dT$_{35}$ concentration. The k_{cat} values for AddA^{H}B and AddA^{H}B^{H} were calculated from independent repeats using saturating concentrations of both dT$_{35}$ and ATP, and the errors shown are the SEM for independent repeats.

and could indicate that AddB is an active ATPase. Nevertheless, an ATPase rate such as that displayed by AddA^{H}B (>1000-fold slower than wild-type) is certainly not commensurate with a role for AddB as a conventional DNA helicase motor, because those proteins typically turnover ATP at ~10–1000/s. Therefore, the ATPase data support the idea that AddA provides the sole motor activity of the AddAB complex.

To further investigate the motor activity of the Walker A mutants we characterized their helicase activity on linearized plasmid DNA substrates (Figure 5A). Reactions were conducted under conditions of limited free magnesium, which are known to suppress the nuclease activity of AddAB and therefore eliminate substrate degradation (37). As expected, wild-type AddAB unwinds the ~3 kb Chi-free substrate, pADGF0, to generate full-length ssDNA (Figure 5A). Substrate processing by AddAB^{H} is indistinguishable from that catalysed by the wild-type enzyme, whereas no substrate unwinding was observed when either of the AddA Walker A mutants were incubated with the DNA substrate as described previously (37). This result further supports the idea that AddA provides the sole motor activity in the AddAB heterodimer. However, we cannot exclude the possibility that AddB possesses a motor activity that is itself dependent on the activity of AddA, for example if a secondary AddB motor operated in series with, and behind, the translocating AddA motor. Such an activity would not easily be detected in the AddA^{H}B mutant enzyme. However, any secondary motor might be expected to influence the rate and/or processivity of the translocating enzyme, as is the case for the RecBCD helicase–nuclease (30). Due to the poor time resolution and relatively short length of the DNA substrate used in gel-based helicase assays, subtle alterations to the rate or processivity may not have been detected. To compare the unwinding rates of wild-type and mutant AddAB complexes we employed the real-time helicase assay (Figure 5B). At saturating concentrations of enzyme, the AddAB^{H} mutant unwound the DNA at a similar rate to wild-type, whereas the AddA^{H}B mutant is completely inactive. The data indicates a slight reduction in the final amplitude of unwinding for the AddAB^{H} mutant, that might indicate a defect in the processivity, or could be caused by other factors such as a slightly increased proportion of non-productive DNA–protein complexes formed before the addition of ATP. A more sensitive test of helicase processivity uses a DNA substrate (such as phage λ) which is comparable in length, or ideally much longer, than the actual processivity of the enzyme. Unwinding of phage λ DNA was analysed by measuring the production of ssDNA with DCC-SSB, and (independently) by recording the displacement of the dsDNA-binding dye Hoechst 33258 by the translocating helicase (dye-displacement assay) (30). In the absence of a trap (i.e. under multiple turnover conditions), AddAB unwinds 16.5 or 18.5 kb of DNA (per DNA-binding site), as measured by the dye-displacement and DCC-SSB assays respectively (Figure 5C). The presence of the trap results in a reduction in the unwinding amplitudes to 14.0 kb (dye) and 12.7 kb (DCC-SSB). This loss of amplitude in a single turnover experiment was also observed for the RecBCD enzyme (30). It could either be due to the trap preventing secondary unwinding of a proportion of the partially-processed reaction products, or might reflect a

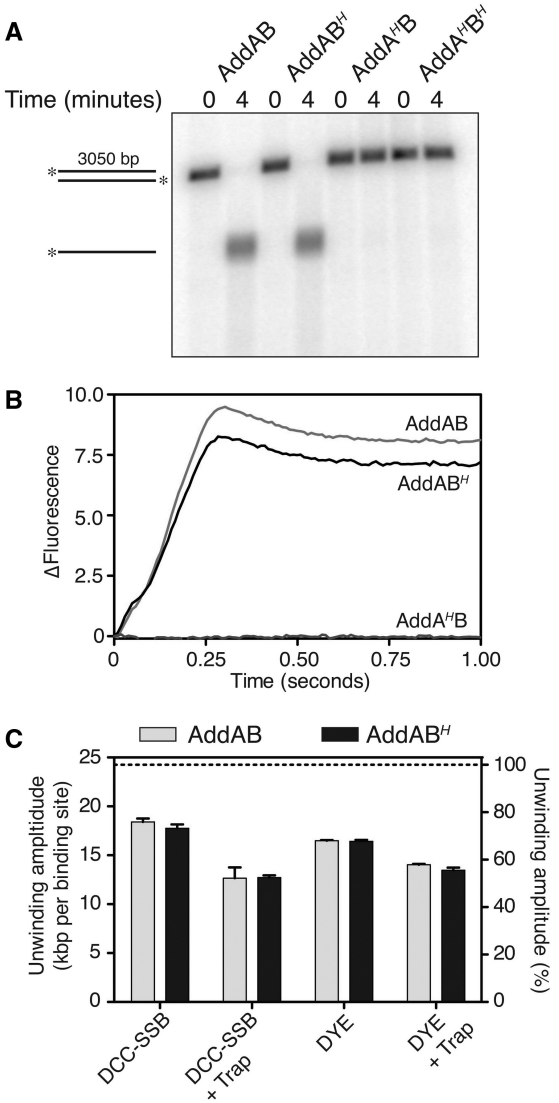

Figure 5. A single helicase motor catalyses processive DNA unwinding by AddAB. (**A**) dsDNA processing by wild-type AddAB and the Walker A mutant enzymes. The processing of the Chi-free DNA substrate pADGF0 was investigated under conditions of limited free magnesium that suppress AddAB nuclease activity. The positions of the dsDNA substrate and the unwound full-length ssDNA reaction products are indicated. (**B**) Comparison of AddAB and AddAB^{H} DNA unwinding using the DCC-SSB helicase assay. The DNA substrate used is shown in Figure 4A. Saturating (2.5 nM) AddAB and AddAB^{H} were pre-bound to 1 nM DNA substrate that was blocked at the distal end with streptavidin. Reactions were initiated with 0.5 mM ATP and 100 nM AddA^{H}B. For the AddA^{H}B trace, the experiment was conducted as described for AddAB and AddAB^{H}, however no helicase was pre-bound to the DNA substrate. The data have been normalized by subtracting the initial fluorescence values for the individual traces. (**C**) Analysis of the processivity of the wild-type AddAB and AddAB^{H}. The proportions of the ~48.5-kb Phage λ DNA molecule unwound by AddAB and AddAB^{H} were measured using the DCC-SSB and dye-displacement assays. The data are the average of at least two repeats and the error bars represent the SEM.

proportion of AddAB enzymes that bind to the substrate in an inactive conformation and require dissociation and rebinding in order to unwind the substrate. Unwinding amplitudes measured in this way are underestimates of the true processivity of AddAB due to the finite length of the DNA substrate, but can be corrected using a model for the unwinding of the phage DNA by two AddAB molecules initiating from each end of the substrate (Supplementary Figure S5 and Table 3). This procedure suggests that the processivity of wild-type AddAB is between 21 and 27 kb or between 14 and 16 kb in the absence or presence of the trap respectively, and depending on the assay used (Table 3). The values for the AddAB^{H} complex are very similar to those of wild-type AddAB (between 21 and 24.5 kb or between 14 and 15 kb in the absence or presence of the trap respectively), demonstrating that the AddB Walker A motif does not contribute significantly to the DNA unwinding processivity. For comparison, inactivation of each single motor in the dual-motor RecBCD enzyme results in processivity decreases of either 6- or 25-fold, measured using the same assays (30).

The AddA subunit is a ssDNA translocase and DNA helicase with 3′→5′ polarity

To assess the DNA translocation and unwinding polarity of the AddA helicase motor, we expressed and purified the AddA subunit of the AddAB complex in isolation. To simplify the interpretation of the results, the D1172A mutation (denoted by an *N*) was also introduced to inactivate the AddA nuclease domain (37). Two mutant enzymes were generated: AddA^{N} and a double mutant AddA^{N,H} that also contains the K36A Walker A mutation that abolishes AddAB ATPase and helicase activities (Figure 5A). To aid purification, the proteins were expressed with N-terminal hexa-histidine tags. Both mutant enzymes displayed identical properties during purification and the final preparations were of equivalent purity (Supplementary Figure S6).

Table 3. Processivity values for wild-type AddAB and AddAB^{H} measured using two different helicase assays

Assay	AddAB Processivity (kb)		AddAB^{H} processivity (kb)	
	Raw[a]	Corrected[b]	Raw	Corrected
Dye	16.50 ± 0.06	20.8	16.43 ± 0.14	20.7
Dye + Trap	14.02 ± 0.09	15.8	13.47 ± 0.26	14.9
DCC-SSB	18.40 ± 0.39	26.4	17.76 ± 0.40	24.3
DCC-SSB + Trap	12.66 ± 1.11	13.7	12.76 ± 0.22	13.8

Experimental λ DNA unwinding amplitudes showing the SEM for independent repeats and corrected processivity values are presented for AddAB and AddAB^{H}.

[a]Raw values refer to measured unwinding amplitudes on phage λ DNA and are underestimates of actual processivity values.

[b]Corrected values are derived from raw values by applying a simple stepping model for the unwinding of the DNA in which two helicases unwind each molecule independently from either end of the substrate (Supplementary Figure S5).

We first investigated the ssDNA translocation properties of AddA using a streptavidin displacement assay (Figure 6A and B) (44). The PcrA and Dda helicases were used as controls for 3′→5′ and 5′→3′ translocation respectively (6,44). As expected, PcrA only displaces streptavidin that is bound at the 5′-end of the ssDNA oligonucleotide, whereas Dda specifically displaces streptavidin from the 3′-end (Figure 6A). Like PcrA, AddA^{N} displaces streptavidin from the 5′-biotinylated oligonucleotide. The reaction requires ATP and is not supported by the AddA^{N,H} mutant protein, demonstrating that the activity is intrinsic to the AddA polypeptide. Omission of free biotin from the reaction prevents the stable dissociation of streptavidin, which eliminates the possibility that we are observing a false positive result due to nucleoytic cleavage of biotin from the DNA substrate. Importantly, AddA^{N} does not catalyse the displacement of streptavidin when the biotin is at the 3′-terminus of the oligonucleotide. We can conclude that AddA translocates on ssDNA with a 3′→5′ polarity and that it is a member of the SF1A mechanistic class (2).

To test if the isolated AddA subunit was capable of unwinding DNA in the absence of AddB, and to confirm the polarity of the putative helicase activity, we employed a strand displacement helicase assay (Figure 6C and D) (45). The assay functions on the basis that many DNA helicases display a preference for unwinding duplex DNA that is flanked either by a 3′- or 5′-terminated ssDNA tail, with the preference reporting on the helicase polarity. The substrates (Supplementary Table S1) consisted of 30-bp duplex region flanked by either a 3′- or 5′-ssDNA tail of 30 bases. An additional substrate consisting only of the 30-bp duplex was used as a control to test for unwinding from free DNA ends or internal sites in the duplex. As in the streptavidin displacement assays, Dda and PcrA served as controls for 5′→3′ and 3′→5′ helicase activity respectively. In line with the previous data (52,53), Dda unwound the 5′-tailed substrate and did not catalyse any unwinding of the 3′-tailed or blunt substrate (Figure 6C). Conversely, PcrA showed a strong preference for the 3′-tailed substrate although some unwinding was detected for both the 5′-tailed and blunt substrates as has been reported (38,54). Like PcrA, AddA^{N} efficiently unwinds the 3′-tailed substrate. The unwinding is dependent on ATP hydrolysis by AddA^{N}, as omitting ATP or inactivating the ATPase activity by mutation abolishes the observed unwinding activity. AddA^{N} catalyses almost no detectable unwinding of either the 5′-tailed or blunt end substrates. These data demonstrate that AddA alone can function as a 3′→5′ DNA helicase, and that the targeting of this activity to DNA ends requires the presence of the AddB subunit.

Mutation of the AddB Walker A motif destabilizes the interaction between AddAB and Chi

Mutation of the AddB Walker A motif does not detectably affect the ATP hydrolysis rate, nor does it decrease the DNA unwinding rate or processivity of the AddAB complex (Figure 5 and Table 2). We next investigated the interaction of this mutant with the recombination

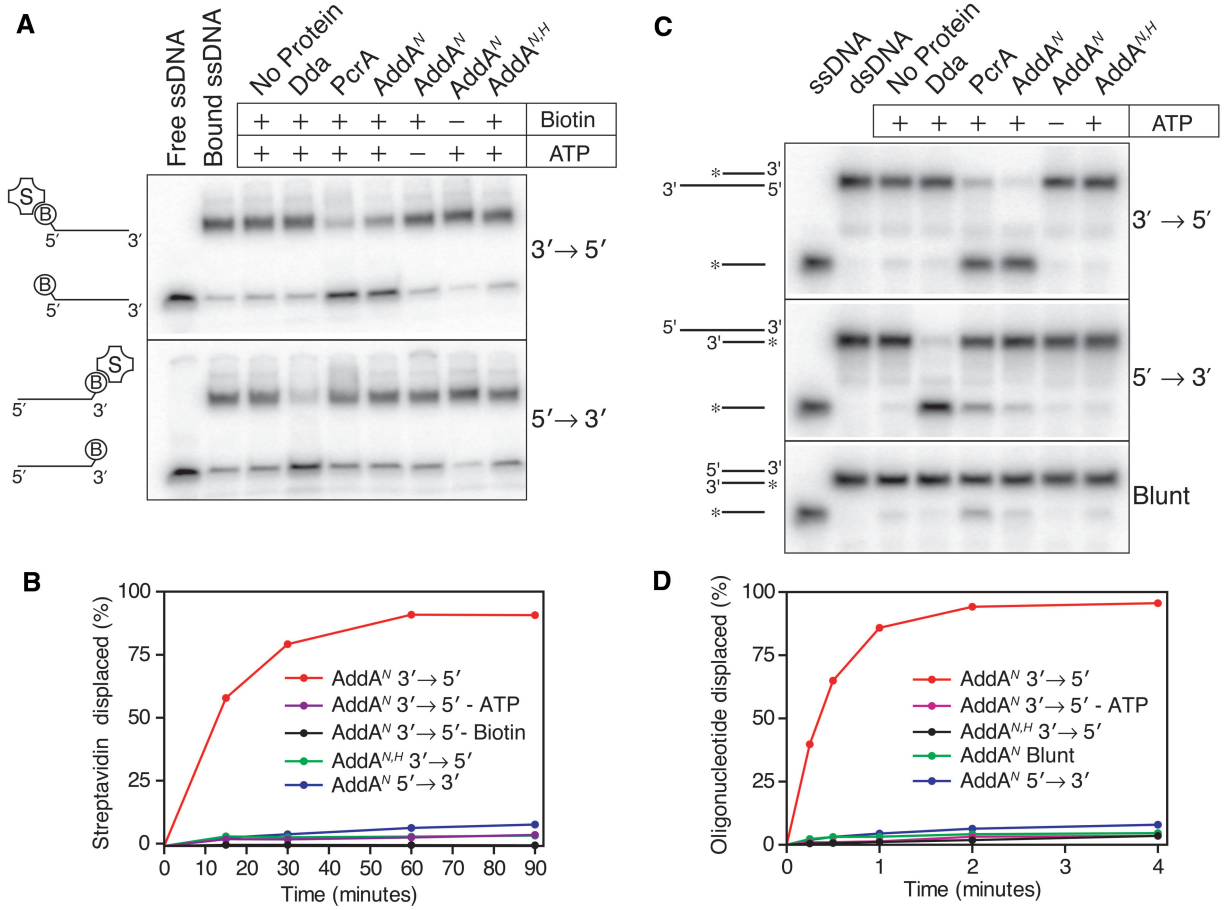

Figure 6. The AddA subunit is a 3′→5′ ssDNA translocase and 3′ → 5′ DNA helicase. (**A**) Streptavidin displacement from 3′- and 5′-biotinylated oligonucleotides. Reactions were conducted at 37°C for 60 min. PcrA and Dda are included as controls for 3′→5′ and 5′→3′ translocation respectively. The positions of the free oligonucleotides and the streptavidin bound oligonucleotides are indicated, as is the translocation directionality that the substrates report on. (**B**) Streptavidin displacement time courses for the various different enzyme and substrate combinations indicated. Reactions were conducted at 37°C and aliquots were removed at the indicated time-points. (**C**) Strand-displacement helicase assays. Reactions were conducted at 20°C for 4 min. Dda and PcrA are included as controls for 5′→3′ and 3′→5′ helicase activity, respectively. The positions of the substrates and displaced oligonucleotides are indicated to the left of the gels, while the polarities on which the substrates report on are indicated to the right. (**D**) Reaction time courses of helicase assays. Reactions were incubated at 20°C and aliquots were withdrawn and quenched at the indicated times. The displaced oligonucleotide is shown as a proportion of the total DNA in each lane.

hotspot Chi. The N-terminal region of AddB that includes the Walker A motif shares weak primary sequence homology with the RecC subunit of *E. coli* RecBCD. The equivalent region of RecC adopts a fold similar to that of a DNA helicase but does not contain any helicase motifs at all (55). Structural and biochemical data suggest that this part of RecC is responsible for the recognition of the *E. coli* Chi sequence (55,56). Based on this comparison with RecC, the AddB Walker A motif might be involved in the Chi-recognition mechanism of the AddAB complex. Indeed, unlike RecBCD, AddAB forms an exceptionally long-lived complex with Chi sequences, and we speculated that this might be stabilized by ATP binding in AddB. The stability of the AddAB-Chi complex can be probed using an exonuclease chase assay. The Chi-terminated ssDNA fragments that are produced by AddAB in a typical *in vitro* DNA end processing assay were previously shown to be highly resistant to degradation by an extrinsic 3′→5′ exonuclease (ExoI) because AddAB remains tightly bound at the Chi sequence near the 3′-terminus (46). Using this approach, we compared the stability of the interaction formed between Chi sequences and either the wild-type or AddAB^H complex by monitoring the susceptibility of Chi-terminated ssDNA fragments to degradation by ExoI. The substrate was 5′-tailed at one end to ensure uni-directional translocation and to maximize the proportion of enzymes that encounter a correctly-orientated Chi sequence. Before ExoI addition, both wild-type AddAB and the AddAB^H mutant enzyme produced Chi-fragments with similar efficiency. Following ExoI addition, the Chi-fragments produced by wild-type AddAB are (as expected) rather stable; the apparent unbinding rate constant is 0.16/min (Figure 7). In contrast, the Chi-fragments produced by AddAB^H are degraded nearly 3-fold faster (at 0.44/min). Therefore, mutation of the AddB Walker A motif weakens the interaction formed between the enzyme complex and the Chi containing DNA. This is consistent with the idea that AddB is involved in Chi recognition, and with the hypothesis that the Walker A motif may function,

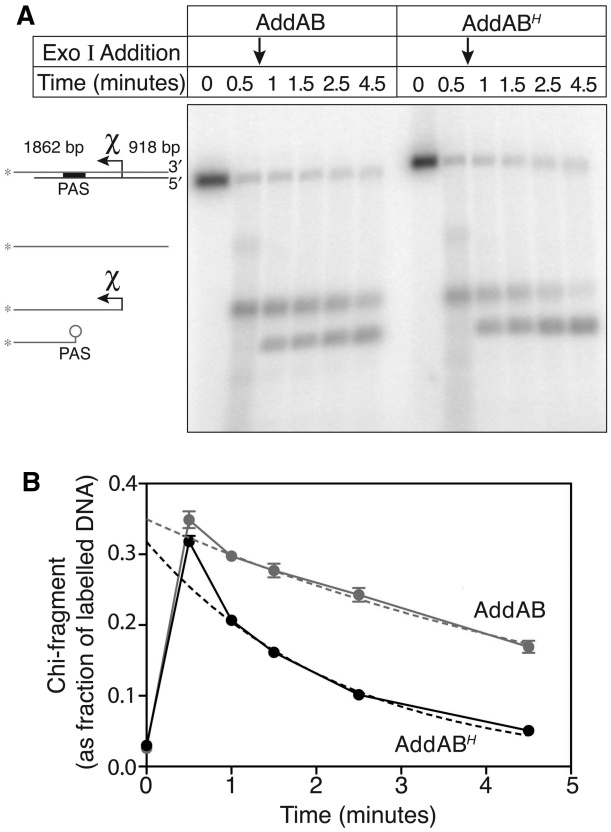

Figure 7. Mutation of the AddB Walker A motif reduces the stability of the AddAB:Chi complex. The stability of the complexes formed between Chi and the AddAB or AddAB^{H} enzymes were investigated using an exonuclease chase experiment. (**A**) Tailed 5′-^{32}P-labelled pAGD6406 (Chi +) (1.6 nM) was incubated with 3.2 nM AddAB in standard high magnesium reaction buffer. Following a 30-s incubation, ExoI was added and aliquots were removed at the indicated times. The positions of the substrate and reaction products are indicated to the left of the gel. The PAS site is a region of secondary structure that is resistant to ExoI degradation. (**B**) The proportions of Chi-fragments remaining at each time point were quantified. The data represents the average of four repeats with the error bars showing the SEM. The dotted lines show fits of the data to a single exponential decrease (forced to decay to zero) to yield apparent unbinding rate constants for the AddAB-Chi fragment interaction. In performing this fit, we are interested in determining the rate of decay of the ExoI-protected (AddAB bound) Chi fragment. Therefore, the 0.5-min sample (which is taken before ExoI chase addition) is taken as an approximation of the 0-min timepoint. This is because the 0.5-min sample measures total Chi fragment (both ExoI-protected and ExoI-sensitive) which is equivalent to the starting yield of ExoI-protected fragment formed within the first few seconds of the reaction. Measurements of the intensity of the Chi band made after the addition of the ExoI chase only reflect ExoI-protected material.

at least in part, to lock the enzyme onto the Chi-containing DNA following Chi-recognition.

DISCUSSION

The AddAB helicase–nuclease was known to be capable of processing DNA molecules in excess of 3000 bp in length (57) but the functional oligomeric state of the AddAB enzyme during dsDNA end-processing has never been directly determined. Furthermore, the primary structure of AddAB indicates that the AddA subunit of the complex harbours a SF1 helicase, whilst a motor function for the AddB subunit cannot be excluded based on primary structure analysis due to the presence of a conserved Walker A motif at the N-terminus. Here we have characterized the oligomeric state of the active AddAB enzyme and determined the number of helicase motors functioning within that complex.

Data from AUC and EMSA assays together show that a single AddAB heterodimer binds to a short DNA substrate. Single turnover helicase assays unequivocally show that a single AddAB heterodimer is capable of processively unwinding a DNA molecule containing a single free end, because the amplitude of DNA unwinding saturates at much greater than 50% when the concentration of AddAB is sufficient to allow the binding of one AddAB molecule. This corroborates the idea that AddAB functions as a heterodimer, as was deduced from a single molecule analysis in which the complex was sparsely immobilized on the surface of a coverslip (41). In agreement with previous work, mutation of the AddA Walker A motif in the AddAB heterodimer essentially abolishes ssDNA-dependent ATPase and helicase activity (37,51). This is mirrored by the results of *in vivo* genetic experiments, which found that the AddA Walker A motif is essential in order to confer wild-type levels of resistance to UV radiation and mitomycin C (58). In contrast, mutation of the AddB Walker A motif does not affect the ATPase, nor does it significantly alter either the helicase rate or processivity of the complex. In common with the AddAB heterodimeric complex (36), the isolated AddA subunit has intrinsic 3′→5′ ssDNA translocation activity and this supports 3′→5′ DNA helicase activity. Taken together, the data demonstrate that the AddAB heterodimer contains a single SF1A helicase motor in the AddA subunit of the complex.

In contrast to AddAB, RecBCD-type helicase–nuclease enzymes employ a bipolar translocation mechanism involving the complementary activities of both a SF1A and a SF1B motor (27,28). Nevertheless, both AddAB and RecBCD are potent helicases, catalysing rapid and processive DNA unwinding. There are several possible explanations for the differing translocation mechanisms employed by RecBCD- and AddAB-type enzymes. Bipolar translocation is required for the maximum processivity of RecBCD and this extreme processivity (~35 kb) might reflect the fact that *E. coli* RecBCD recognizes an octameric Chi sequence that, despite being over represented, occurs on average only every 5000 bp (30). In the case of *B. subtilis* AddAB, the enzyme responds to a far more abundant pentameric Chi sequence (57), implying that AddAB-type enzymes may not need to be as processive as their RecBCD counterparts. Therefore, the finding that AddAB has a processivity in the region of 20 kb on λ DNA suggests that there may not be a strong correlation between the length of a Chi sequence and helicase–nuclease processivity. Note however that the processivity value for AddAB should be viewed with some caution in this context, as the λ DNA substrate contains multiple *B. subtilis* Chi sequences and therefore the assay does not report specifically on AddAB processivity prior

to Chi-recognition. The RexAB (equivalent to AddAB) complex from *Lactococcus lactis* recognizes a heptameric Chi sequence (59), presumably giving the enzyme a more similar processivity requirement to *E. coli* RecBCD, despite its probable single motor organization. Recently, an AddAB homologue from *Bacteroides fragilis* was shown to unwind (on average) 14 kb of DNA per binding event, but the Chi recognition sequence for this enzyme is unknown (48). More helicase–nuclease complexes will need to be characterized in order to establish any link between processivity and Chi sequence abundance. Bipolar translocation has also been suggested to help RecBCD unwind DNA through sites of lesions and protein road blocks (30). This may indeed be the case, but it seems unlikely that such an advantage would only be important in a sub-set of bacteria where RecBCD rather than AddAB predominates. Perhaps the requirement of a second motor in RecBCD reflects the fact that the enzyme has a single nuclease active site. Bipolar translocation feeds both nascent single strands of DNA to the rear of the enzyme such that both strands are cleaved by a single nuclease domain (55). In contrast, AddAB-type enzymes have two nuclease domains that are each responsible for cleavage of one of the nascent single-strands and coordinating their exit may be less critical.

It has recently been reported that a third distinct class of helicase–nuclease enzyme exists in the *Actinomycetales* bacteria (60). The complex that was identified in *Mycobacterium smegmatis*, consists of two subunits and has been named AdnAB. The AdnB subunit is homologous to *B. subtilis* AddA. AdnA has a C-terminal nuclease domain that is homologous to the AddB nuclease, whilst the N-terminus appears to harbour most or all of the SF1 helicase motifs (60). The domain organization of AdnAB presents the intriguing possibility that, unlike either AddAB or RecBCD, this complex may contain two nuclease and two helicase domains. However, it is not currently clear that both putative motor domains of AdnAB are active. Indeed, mutagenesis of either the AdnA or AdnB Walker A motifs gives a similar result to the mutagenesis studies presented here for AddAB. Mutation of AdnB abolishes DNA-stimulated ATPase, $3'\rightarrow5'$ ssDNA translocation and dsDNA unwinding activities, whilst mutation of AdnA has only a minor effect (60,61).

Several SF1 helicase enzymes display little or no DNA unwinding activity as monomeric species, leading to suggestions that a single SF1 motor is not sufficient to catalyse processive DNA unwinding (11–16). Instead, models have been proposed whereby helicases function as either dimeric complexes, or as co-operating monomers (Figure 1) (12,13,15,16). These enzymes have largely been studied in isolation, despite the fact that, like AddA, many of them interact physically and/or functionally with specific partner proteins or protein co-factors (such as SSB) *in vivo* (19,20,22,23,62). The AddAB enzyme serves as an interesting model for studying helicase activity *in vitro*. The AddA SF1 helicase motor forms a stable complex with its partner protein (AddB), and this purified complex catalyses a DNA end processing reaction that closely reflects its known *in vivo* function, enabling the motor activity to be studied in a biologically relevant context. Essentially, the AddA motor of the complex is 'monomeric' in the sense that it does not require an interaction with a second active SF1 helicase motor to display optimum helicase activity. The AddB polypeptide is not required for this motor activity, but is essential for the targeting of the helicase activity to free DNA ends, which are the physiological substrate for AddAB. Our data show that another key role for AddB is in the process of Chi-recognition, because mutation of its conserved Walker A motif destabilizes the complex formed between the AddAB complex and Chi. Therefore, AddB likely plays a similar 'Chi-scanning' role to that suggested for RecC in the RecBCD complex (55) but with the intriguing twist that the process may be dependent on ATP binding in AddB. This idea will be tested in future work. In any case, it is clear that the architecture of the whole AddAB complex is critical in modifying the AddA helicase to perform a specialized role in DNA break processing.

Based upon these studies of the AddAB complex, and previous analyses of the TraI and PcrA:RepD systems (23,24), we conclude that the underlying mechanism for SF1 helicase activity does not require functional or physical interactions between multiple helicase motor domains. The apparent need for such interactions in related SF1 enzymes may either reflect a specific aspect of their cellular function for which multimerization is necessary, or the lack of critical trans-acting factors such as accessory proteins or protein co-factors *in vitro*.

SUPPLEMENTARY DATA

Supplementary Data are available at NAR Online.

ACKNOWLEDGEMENTS

The authors are grateful to Neville Gilhooly and Dr Fernando Moreno-Herrero for their comments on the article, and thank Alap Chavda and Caroline Morris for synthesis of DCC-SSB.

FUNDING

European Research Council (206117-2); the Wellcome Trust (077368); the Medical Research Council (U117512742 to M.R.W.); Biotechnology and Biological Sciences Research Council studentship (to J.T.P.Y.); Royal Society University Research Fellowship (to M.S.D.). Funding for open access charge: Wellcome Trust.

Conflict of interest statement. None declared.

REFERENCES

1. Gorbalenya,A.E. and Koonin,E.V. (1993) Helicases - amino-acid-sequence comparisons and structure-function-relationships. *Curr. Opin. Struct. Biol.*, **3**, 419–429.

2. Singleton,M.R., Dillingham,M.S. and Wigley,D.B. (2007) Structure and mechanism of helicases and nucleic acid translocases. *Annu. Rev. Biochem.*, **76**, 23–50.
3. Subramanya,H.S., Bird,L.E., Brannigan,J.A. and Wigley,D.B. (1996) Crystal structure of a DExx box DNA helicase. *Nature*, **384**, 379–383.
4. Kim,J.L., Morgenstern,K.A., Griffith,J.P., Dwyer,M.D., Thomson,J.A., Murcko,M.A., Lin,C. and Caron,P.R. (1998) Hepatitis C virus NS3 RNA helicase domain with a bound oligonucleotide: the crystal structure provides insights into the mode of unwinding. *Structure*, **6**, 89–100.
5. Singleton,M.R. and Wigley,D.B. (2002) Modularity and specialization in superfamily 1 and 2 helicases. *J. Bacteriol.*, **184**, 1819–1826.
6. Dillingham,M.S., Wigley,D.B. and Webb,M.R. (2000) Demonstration of unidirectional single-stranded DNA translocation by PcrA helicase: measurement of step size and translocation speed. *Biochemistry*, **39**, 205–212.
7. Lee,J.Y. and Yang,W. (2006) UvrD helicase unwinds DNA one base pair at a time by a two-part power stroke. *Cell*, **127**, 1349–1360.
8. Velankar,S.S., Soultanas,P., Dillingham,M.S., Subramanya,H.S. and Wigley,D.B. (1999) Crystal structures of complexes of PcrA DNA helicase with a DNA substrate indicate an inchworm mechanism. *Cell*, **97**, 75–84.
9. Soultanas,P., Dillingham,M.S., Wiley,P., Webb,M.R. and Wigley,D.B. (2000) Uncoupling DNA translocation and helicase activity in PcrA: direct evidence for an active mechanism. *EMBO J.*, **19**, 3799–3810.
10. Saikrishnan,K., Powell,B., Cook,N.J., Webb,M.R. and Wigley,D.B. (2009) Mechanistic basis of 5′-3′ translocation in SF1B helicases. *Cell*, **137**, 849–859.
11. Ha,T., Rasnik,I., Cheng,W., Babcock,H.P., Gauss,G.H., Lohman,T.M. and Chu,S. (2002) Initiation and re-initiation of DNA unwinding by the Escherichia coli Rep helicase. *Nature*, **419**, 638–641.
12. Brendza,K.M., Cheng,W., Fischer,C.J., Chesnik,M.A., Niedziela-Majka,A. and Lohman,T.M. (2005) Autoinhibition of Escherichia coli Rep monomer helicase activity by its 2B subdomain. *Proc. Natl Acad. Sci. USA*, **102**, 10076–10081.
13. Byrd,A.K. and Raney,K.D. (2005) Increasing the length of the single-stranded overhang enhances unwinding of duplex DNA by bacteriophage T4 Dda helicase. *Biochemistry*, **44**, 12990–12997.
14. Niedziela-Majka,A., Chesnik,M.A., Tomko,E.J. and Lohman,T.M. (2007) Bacillus stearothermophilus PcrA monomer is a single-stranded DNA translocase but not a processive helicase in vitro. *J. Biol. Chem.*, **282**, 27076–27085.
15. Yang,Y., Dou,S.X., Ren,H., Wang,P.Y., Zhang,X.D., Qian,M., Pan,B.Y. and Xi,X.G. (2008) Evidence for a functional dimeric form of the PcrA helicase in DNA unwinding. *Nucleic Acids Res.*, **36**, 1976–1989.
16. Maluf,N.K., Fischer,C.J. and Lohman,T.M. (2003) A Dimer of Escherichia coli UvrD is the active form of the helicase in vitro. *J. Mol. Biol.*, **325**, 913–935.
17. Nanduri,B., Byrd,A.K., Eoff,R.L., Tackett,A.J. and Raney,K.D. (2002) Pre-steady-state DNA unwinding by bacteriophage T4 Dda helicase reveals a monomeric molecular motor. *Proc. Natl Acad. Sci. USA*, **99**, 14722–14727.
18. Lohman,T.M., Tomko,E.J. and Wu,C.G. (2008) Non-hexameric DNA helicases and translocases: mechanisms and regulation. *Nat. Rev. Mol. Cell. Biol.*, **9**, 391–401.
19. Atkinson,J., Guy,C.P., Cadman,C.J., Moolenaar,G.F., Goosen,N. and McGlynn,P. (2009) Stimulation of UvrD helicase by UvrAB. *J. Biol. Chem.*, **284**, 9612–9623.
20. Matson,S.W. and Robertson,A.B. (2006) The UvrD helicase and its modulation by the mismatch repair protein MutL. *Nucleic Acids Res.*, **34**, 4089–4097.
21. Arai,N. and Kornberg,A. (1981) Rep protein as a helicase in an active, isolatable replication fork of duplex phi X174 DNA. *J. Biol. Chem.*, **256**, 5294–5298.
22. Soultanas,P., Dillingham,M.S., Papadopoulos,F., Phillips,S.E., Thomas,C.D. and Wigley,D.B. (1999) Plasmid replication initiator protein RepD increases the processivity of PcrA DNA helicase. *Nucleic Acids Res.*, **27**, 1421–1428.
23. Slatter,A.F., Thomas,C.D. and Webb,M.R. (2009) PcrA helicase tightly couples ATP hydrolysis to unwinding double-stranded DNA, modulated by the initiator protein for plasmid replication, RepD. *Biochemistry.*, **48**, 6326–6334.
24. Sikora,B., Eoff,R.L., Matson,S.W. and Raney,K.D. (2006) DNA unwinding by Escherichia coli DNA helicase I (TraI) provides evidence for a processive monomeric molecular motor. *J. Biol. Chem.*, **281**, 36110–36116.
25. Dillingham,M.S. and Kowalczykowski,S.C. (2008) RecBCD enzyme and the repair of double-stranded DNA breaks. *Microbiol. Mol. Biol. Rev.*, **72**, 642–671.
26. Yeeles,J.T. and Dillingham,M.S. (2010) The processing of double-stranded DNA breaks for recombinational repair by helicase-nuclease complexes. *DNA Repair*, **9**, 276–285.
27. Dillingham,M.S., Spies,M. and Kowalczykowski,S.C. (2003) RecBCD enzyme is a bipolar DNA helicase. *Nature*, **423**, 893–897.
28. Taylor,A.F. and Smith,G.R. (2003) RecBCD enzyme is a DNA helicase with fast and slow motors of opposite polarity. *Nature*, **423**, 889–893.
29. Bianco,P.R., Brewer,L.R., Corzett,M., Balhorn,R., Yeh,Y., Kowalczykowski,S.C. and Baskin,R.J. (2001) Processive translocation and DNA unwinding by individual RecBCD enzyme molecules. *Nature*, **409**, 374–378.
30. Dillingham,M.S., Webb,M.R. and Kowalczykowski,S.C. (2005) Bipolar DNA translocation contributes to highly processive DNA unwinding by RecBCD enzyme. *J. Biol. Chem.*, **280**, 37069–37077.
31. Roman,L.J., Eggleston,A.K. and Kowalczykowski,S.C. (1992) Processivity of the DNA helicase activity of Escherichia coli recBCD enzyme. *J. Biol. Chem.*, **267**, 4207–4214.
32. Roman,L.J. and Kowalczykowski,S.C. (1989) Characterization of the helicase activity of the Escherichia coli RecBCD enzyme using a novel helicase assay. *Biochemistry*, **28**, 2863–2873.
33. Taylor,A.F. and Smith,G.R. (1995) Monomeric RecBCD enzyme binds and unwinds DNA. *J. Biol. Chem.*, **270**, 24451–24458.
34. Chedin,F. and Kowalczykowski,S.C. (2002) A novel family of regulated helicases/nucleases from Gram-positive bacteria: insights into the initiation of DNA recombination. *Mol. Microbiol.*, **43**, 823–834.
35. Cromie,G.A. (2009) Phylogenetic ubiquity and shuffling of the bacterial RecBCD and AddAB recombination complexes. *J. Bacteriol.*, **191**, 5076–5084.
36. Yeeles,J.T., Cammack,R. and Dillingham,M.S. (2009) An iron-sulfur cluster is essential for the binding of broken DNA by AddAB-type helicase-nucleases. *J. Biol. Chem.*, **284**, 7746–7755.
37. Yeeles,J.T. and Dillingham,M.S. (2007) A Dual-nuclease mechanism for DNA break processing by AddAB-type helicase-nucleases. *J. Mol. Biol.*, **371**, 66–78.
38. Bird,L.E., Brannigan,J.A., Subramanya,H.S. and Wigley,D.B. (1998) Characterisation of Bacillus stearothermophilus PcrA helicase: evidence against an active rolling mechanism. *Nucleic Acids Res.*, **26**, 2686–2693.
39. Dillingham,M.S., Tibbles,K.L., Hunter,J.L., Bell,J.C., Kowalczykowski,S.C. and Webb,M.R. (2008) Fluorescent single-stranded DNA binding protein as a probe for sensitive, real-time assays of helicase activity. *Biophys. J.*, **95**, 3330–3339.
40. Webb,M.R. (2003) In. In Johnson,K.A. (ed.), *Kinetic Analysis: A Practical Approach*. Oxford University Press, Oxford, pp. 131–152.
41. Fili,N., Mashanov,G.I., Toseland,C.P., Batters,C., Wallace,M.I., Yeeles,J.T.P., Dillingham,M.S., Webb,M.R. and Molloy,J.E. (2010) Visualizing helicases unwinding DNA at the single molecule level. *Nucleic Acids Res.*, **38**, 4448–4457.
42. Yeeles,J.T.P. (2009) The initiation of double-stranded DNA break repair by an AddAB-type helicase-nuclease. PhD thesis, University of Bristol, Bristol.
43. Harding,S.E., Rowe,A.J. and Horton,J.C. (1992) *Analytical Ultracentrifugation in Biochemistry and Polymer Science*. Royal Society of Chemistry, Cambridge, England.
44. Morris,P.D. and Raney,K.D. (1999) DNA helicases displace streptavidin from biotin-labeled oligonucleotides. *Biochemistry*, **38**, 5164–5171.

45. Matson,S.W., Tabor,S. and Richardson,C.C. (1983) The gene 4 protein of bacteriophage T7. Characterization of helicase activity. *J. Biol. Chem.*, **258**, 14017–14024.
46. Chedin,F., Handa,N., Dillingham,M.S. and Kowalczykowski,S.C. (2006) The AddAB helicase/nuclease forms a stable complex with its cognate chi sequence during translocation. *J. Biol. Chem.*, **281**, 18610–18617.
47. Kunzelmann,S., Morris,C., Chavda,A.P., Eccleston,J.F. and Webb,M.R. (2010) Mechanism of interaction between single-stranded DNA binding protein and DNA. *Biochemistry*, **49**, 843–852.
48. Reuter,M., Parry,F., Dryden,D.T. and Blakely,G.W. (2010) Single-molecule imaging of Bacteroides fragilis AddAB reveals the highly processive translocation of a single motor helicase. *Nucleic Acids Res.*, **38**, 3721–3731.
49. Soultanas,P., Dillingham,M.S., Velankar,S.S. and Wigley,D.B. (1999) DNA binding mediates conformational changes and metal ion coordination in the active site of PcrA helicase. *J. Mol. Biol.*, **290**, 137–148.
50. Brune,M., Hunter,J.L., Corrie,J.E. and Webb,M.R. (1994) Direct, real-time measurement of rapid inorganic phosphate release using a novel fluorescent probe and its application to actomyosin subfragment 1 ATPase. *Biochemistry*, **33**, 8262–8271.
51. Haijema,B.J., Meima,R., Kooistra,J. and Venema,G. (1996) Effects of lysine-to-glycine mutations in the ATP-binding consensus sequences in the AddA and AddB subunits on the Bacillus subtilis AddAB enzyme activities. *J. Bacteriol.*, **178**, 5130–5137.
52. Raney,K.D. and Benkovic,S.J. (1995) Bacteriophage T4 Dda helicase translocates in a unidirectional fashion on single-stranded DNA. *J. Biol. Chem.*, **270**, 22236–22242.
53. Jongeneel,C.V., Formosa,T. and Alberts,B.M. (1984) Purification and characterization of the bacteriophage T4 dda protein. A DNA helicase that associates with the viral helix-destabilizing protein. *J. Biol. Chem.*, **259**, 12925–12932.
54. Anand,S.P. and Khan,S.A. (2004) Structure-specific DNA binding and bipolar helicase activities of PcrA. *Nucleic Acids Res.*, **32**, 3190–3197.
55. Singleton,M.R., Dillingham,M.S., Gaudier,M., Kowalczykowski,S.C. and Wigley,D.B. (2004) Crystal structure of RecBCD enzyme reveals a machine for processing DNA breaks. *Nature*, **432**, 187–193.
56. Arnold,D.A., Handa,N., Kobayashi,I. and Kowalczykowski,S.C. (2000) A novel, 11 nucleotide variant of chi, chi*: one of a class of sequences defining the Escherichia coli recombination hotspot chi. *J. Mol. Biol.*, **300**, 469–479.
57. Chedin,F., Ehrlich,S.D. and Kowalczykowski,S.C. (2000) The Bacillus subtilis AddAB helicase/nuclease is regulated by its cognate Chi sequence in vitro. *J. Mol. Biol.*, **298**, 7–20.
58. Haijema,B.J., Noback,M., Hesseling,A., Kooistra,J., Venema,G. and Meima,R. (1996) Replacement of the lysine residue in the consensus ATP-binding sequence of the AddA subunit of AddAB drastically affects chromosomal recombination in transformation and transduction of Bacillus subtilis. *Mol. Microbiol.*, **21**, 989–999.
59. el Karoui,M., Ehrlich,D. and Gruss,A. (1998) Identification of the lactococcal exonuclease/recombinase and its modulation by the putative Chi sequence. *Proc. Natl Acad. Sci. USA*, **95**, 626–631.
60. Sinha,K.M., Unciuleac,M.C., Glickman,M.S. and Shuman,S. (2009) AdnAB: a new DSB-resecting motor-nuclease from mycobacteria. *Genes Dev.*, **23**, 1423–1437.
61. Unciuleac,M.C. and Shuman,S. (2010) Characterization of the mycobacterial AdnAB DNA motor provides insights into the evolution of bacterial motor-nuclease machines. *J. Biol. Chem.*, **285**, 2632–2641.
62. Chao,K.L. and Lohman,T.M. (1991) DNA-induced dimerization of the Escherichia coli Rep helicase. *J. Mol. Biol.*, **221**, 1165–1181.
63. Harding,S. (1994) In. In Jones,C., Mulloy,B. and Thomas,A.H. (eds), *Microscopy, Optical Spectroscopy, and Macroscopic Techniques*, Vol. 22. Humana Press, Totawa, pp. 75–84.